

Fatigue performance of rib-roof weld in steel bridge decks with corner braces

Zhongqiu Fu^a, Bohai Ji^{*}, Yixun Wang^b and Jie Xu^c

College of Civil and Transportation Engineering, Hohai University, 1 Xikang Rd., Nanjing, Jiangsu 210098, P.R. China

(Received June 26, 2017, Revised September 3, 2017, Accepted September 29, 2017)

Abstract. To study the effects of corner braces on fatigue performance of the *U*-rib and roof weld in steel bridge decks, the fatigue experiment was carried out to compare characteristics of the crack shape with and without corner braces. The improvement of fatigue life and stress variation after setting corner braces were also analysed. Different parameters of corner brace sizes, arrangements, and detail types were considered in the FEM models to obtain stress distribution and variation at the weld. Furthermore, enhancement of the fatigue performance by corner braces was evaluated. The results demonstrated that the corner brace could improve the fatigue life of the *U*-rib and roof weld, which exerted even no influence on the crack shape. Moreover, stress of the roof weld was decreased and the crack position was transferred from the root weld to *U*-rib and corner brace weld. It was suggested no weld scallop should be drilled on the corner brace. A transverse rib with lower height which was set between *U*-ribs was favourable for improvement of fatigue performance.

Keywords: steel bridge deck; weld fatigue; corner brace; stress distribution; construction detail

1. Introduction

Due to their current structural characteristics, fatigue cracks in orthotropic steel decks are inevitable and they affect the service life of such bridges (Saber *et al.* 2016, Guo and Chen 2013). These cracks are difficult to detect in their initial stages and they grow rapidly. Penetrating cracks cause damage to the pavement before the design life and corrosion of the steel girder become limiting factors (Krejsa *et al.* 2016, Kainuma *et al.* 2016). The detection of bridge fatigue cracks is onerous and has limited accuracy: the cost of repairing such cracks is high while the efficacy of any repairs needs to be improved (Xie *et al.* 2015, Sakagami 2015). From a mechanical perspective, a reduction in stress concentration can improve the fatigue performance (Ilman *et al.* 2016, Fan *et al.* 2016) and postpone the appearance of cracks, including decreasing the number of defects, weakening the geometrical shape mutations arising therefrom, and regulating the residual stress distribution. However, the local stress distribution in the structure remains unchanged due to the same local stiffness of the deck prevailing. Thus, the cracking problem cannot be resolved in any fundamental sense. Meanwhile, changes in the stiffness distribution across typical structural details can optimise the stress distribution.

Fatigue cracks in an orthotropic steel deck are mainly caused by large differential deformation in different deck directions because of the local stiffness distribution therein. The methods used to increase the local stiffness and postpone cracking were studied. Application of steel fiber reinforced concrete (SFRC) in the deck pavement was proved effective in enhancing the deck stiffness (Kolase and Desai 2015). Reinforced high-performance concrete (RHPC) was also proposed for application in such bridge pavements (De and Kolseim 2015). Light material pavements were proposed to reduce the self-weight but also decrease the local stress amplitude: some suggestions involved use of reactive powder concrete (RPC) (Shao *et al.* 2013). Although the application of high-performance pavements was able to enhance bridge fatigue performance, the improvement was caused by external changes to the deck. Therefore, the methods of changing local structure details were adopted in engineering practice, such as shape changes at holes in the cross-beam below the *U*-rib and increases in roof thickness. Different accessories were proposed, including application of opening rib (Zhang *et al.* 2016), the addition of a clapboard in the *U*-rib and in-filling with concrete to a part of the *U*-rib. Other methods of structural strengthening were also proposed, and studied, to improve weld fatigue performance (Colombi and Fava 2016, Aljabar *et al.* 2016).

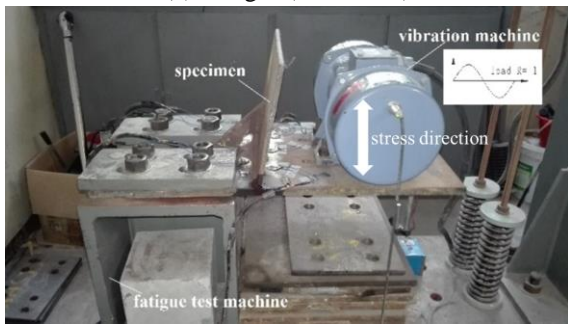
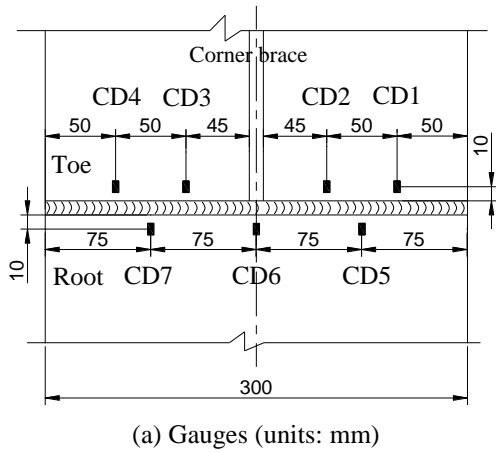
The great stiffness difference of material in various directions is the leading cause of roof cracks in steel bridge deck. The setting of corner braces at the weakest position on the *U*-rib and roof weld, which is equivalent to transverse stiffener, can change the local stiffness for improvement of stress distribution. The corner brace can be adopted in the design phase to optimise the stress distribution. It can also be applied in the position with the largest stress amplitude in any operational phase of the bridge life as a measure to postpone the crack propagation.

*Corresponding author, Professor
E-mail: hbbhji@163.com

^aAssociate Professor
E-mail: fumidaut@163.com

^bMaster Student
E-mail: 531849819@qq.com

^cMaster Student
E-mail: 1440909170@qq.com



(b) Loading machine
 Fig. 2 Measuring and loading arrangements

points were arranged at positions 10 mm from the weld toe and root (Fig. 2(a)).

Specimens were tested by mechanical fatigue test machine (Fig. 2(b)) (Yang *et al.* 2016). The specimen was fixed to the machine frame with high-strength bolts, which formed a cantilever arrangement. The cantilever end was connected to the eccentric vibration machine which output a sinusoidal cyclic load with constant amplitude during testing. The stress ratio was set as $R=-1$. The frequency and loading of the machine could be regulated and a counter was available to constantly record the number of loading cycles, which was equal to monitor readings *100.

The measure points couldn't be set on the middle of weld toe where the corner brace was welded, thus the reference point CD6, which was shown in Fig. 2(b), was located on the middle of weld root. The specimens were all loaded under a stress amplitude of 100 MPa at the weld root. Because the stress amplitude was controlled by loading frequency and an accurate value couldn't be accessed, the actual stress amplitude hovered around 10% of the design value. The test was completed when one of the following two conditions occurred: either the crack reached 70% depth of the deck thickness (Fu *et al.* 2017b) or 10 million load cycles had been reached.

3. Discussion of test results

3.1 Crack sections

The specimens were cut along the crack to obtain crack

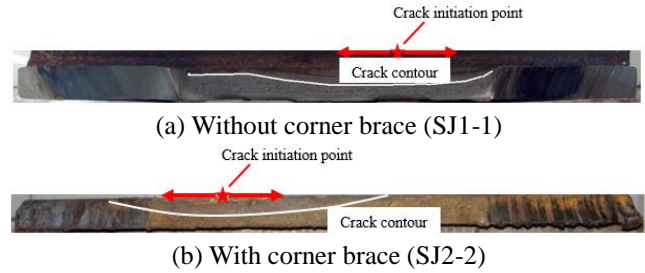


Fig. 3 Crack sections

Table 2 Variation in stress amplitude (SJ2-2)

Weld position	Gauge number	Stress amplitude values				Superposition (MPa)
		Initial (MPa)	Failure (MPa)	Variation (MPa)	Variation rate (%)	
Toe	CD1	72.5	77.2	4.7	6.5	-0.5
	CD2	67.2	49.7	-17.5	-26.0	
	CD3	67.0	72.9	5.9	8.8	
	CD4	74.8	81.2	6.4	8.6	
Root	CD5	79.3	65.5	-13.8	-18.7	0.7
	CD6	97.4	104.9	7.5	5.9	
	CD7	81.6	88.6	7.0	9.6	

cross-sections as shown in Fig. 3. The crack contour was deep in the middle, shallow at both sides, and appeared as a prolate arc. A radial texture appeared on the crack cross-section which was caused by the repeated extrusion on the crack cross-section during fatigue loading. The crack contour of the specimen with a corner brace (SJ2-2) was similar to that of the specimen without a corner brace (SJ1-1). Depths of the cracks in the middle of the section were similar and thus, a corner brace had less effect on the shape of the crack cross-section.

3.2 Stress variation

The crack length of specimen SJ2-3 with the corner brace was less than 100mm when it came to 10 million load cycles. Besides, the fatigue failure occurred quickly after crack initiation in specimen SJ2-1, thus time history of stress variation was too short to be analysed. Therefore, take specimen SJ2-2 for instance and the stress amplitude variations were listed in Table 2. The initial stress amplitude of the reference point (CD6) was 97.4 MPa and agreed with test expectations. The average initial stress amplitude of measuring points near the weld toe (CD1 to CD4) was 70.4 MPa, which was 27.2% lower than the reference stress amplitude. Besides, the average initial stress amplitude near the weld root (CD5 to CD7) were 86.1 MPa and 13.9% lower than the reference stress amplitude. The corner brace enhanced the local stiffness and was set on the weld toe, thus the initial stress amplitude and average stress amplitude of each measuring point at weld toe were much lower than those at weld root. The failed specimen SJ2-2 had a 100 mm length crack at the root near gauge CD5 and a 20 mm length crack at the toe near gauge CD2. The cracks caused some stress redistribution. The failure stress amplitude of CD2 and CD5 significantly decreased

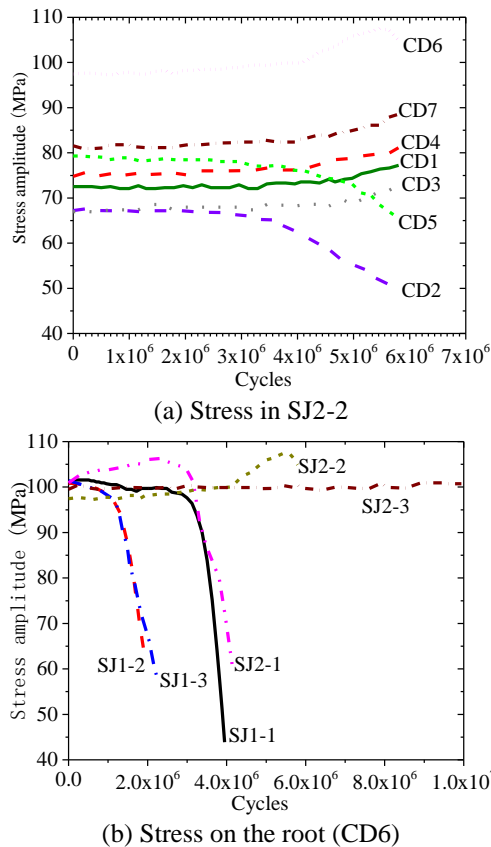


Fig. 4 Stress amplitude variations of specimens

by 26% and 18.7%, respectively. Moreover, the stress amplitudes increased at other measuring points nearby. The stress amplitude variations at weld toe and root, corresponding to the variations at CD1 to CD4, and CD5 to CD7, in Table 2, were superimposed respectively and the results were -0.5 MPa and 0.7 MPa which were both close to zero. The sums demonstrated that the stress redistribution caused by cracking had no effect on the overall bearing capacity of the weld.

Fig. 4 shows the stress amplitudes variation curves under different numbers of loading cycles. From Figure 4(a), the stress amplitudes at CD2 and CD5 had a decreasing trend while other measuring gauges showed an increasing trend. The cracks near CD2 and CD5 cut off the transfer of stress and resulted in the stress amplitude decreasing near the crack and increasing at other locations because of the stress redistribution therein. The stress amplitude variation at CD6 differed from that found elsewhere. Before the crack reached CD6, the stress amplitude increased due to stress redistribution; however, the stress amplitude decreased when the crack reached CD6. Therefore, the stress amplitude showed an increasing trend in the beginning and then a downward trend thereafter.

As shown in Fig. 4(b), stress amplitude variations at the controlling measuring gauge (CD6) were compared to study the effects of a corner brace on the stress amplitude; because the cracking initiation conditions were different, the stress amplitude in different specimens showed different trends. For specimens without corner braces, the stress

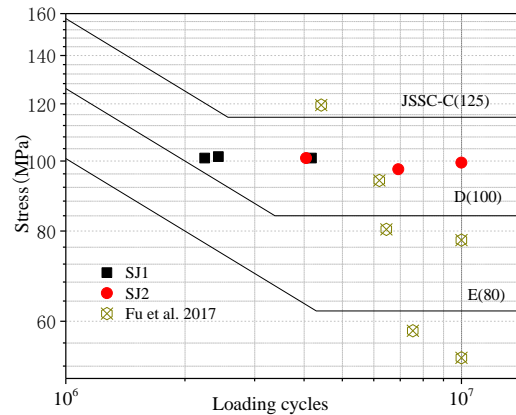


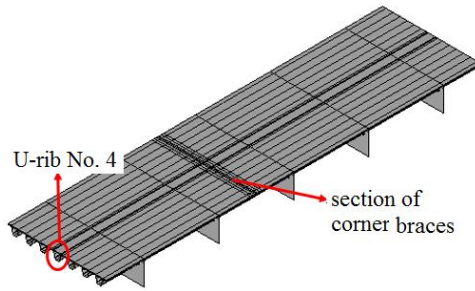
Fig. 5 Mesh grid of topographic model

amplitudes decreased rapidly after the onset of cracking and the stress redistribution was obvious. However, for specimens with corner braces, the stress amplitude variation lagged behind that of specimens without corner braces. Therefore, corner braces improved the stress distribution after the cracking, which improved the fatigue performance.

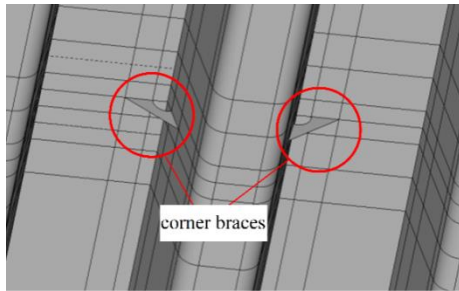
3.3 Fatigue life

In the fatigue tests, the initial stress amplitude at CD6 near the weld root was adopted as the nominal stress amplitude. Fatigue life test results are listed in Table 1. All specimens without corner braces (SJ1) cracked and had shorter fatigue lives. However, fatigue lives of specimens with corner braces (SJ2) were longer. The number of loading cycles applied to SJ2-1 and SJ2-2 were 4,047,800 and 6,920,400 when the cracks length reached 100 mm, respectively. The crack of SJ2-3 was only 10 mm long upon the application of 10 million load cycles.

Referring to the S-N curves of similar fatigue details in the Japanese fatigue design guidelines for steel highway bridges (JSSC) (Japan Road Association), the test results were compared with the specimens setting no corner braces under stress amplitude of 55 MPa and 80 MPa by Fu *et al.* (2017), which were shown in Fig. 5. The loading amplitude of specimens with corner braces was higher than that of Fu *et al.* (2017) but the fatigue life of specimens with corner braces was no less than that of Fu *et al.* (2017) as a whole, implying that the corner brace was positive to enhance the fatigue performance of *U*-rib and roof weld. In Table 1, the average fatigue life of specimens without corner braces was 2,950,067 cycles and that of specimens with corner braces was 6,989,400 cycles (the fatigue life of SJ2-3 was assumed to be a conservative 10 million cycles). The average fatigue life increased by 36.9% because of the use of corner braces. Although the fatigue life of SJ1-1 was similar to that of SJ2-1, it still had a potential to be enhanced because the fatigue experiment was discrete. Besides, the fatigue life was similar among specimens without corner braces but showed a huge diversity among the corner brace specimens. By observing the crack initiation locations, those specimens with corner braces had overlaps from where cracking was initiated, while those specimens without corner braces had no overlaps. Therefore, the corner braces improved the



(a) Steel deck



(b) Corner brace

Fig. 6 FEM models

fatigue performance but it was adversely affected by the overall welding quality. The stress concentration, residual stress and distortion produced by welding defects would reduce the fatigue performance of this detail, thereby weakening the role of corner braces.

4. Finite element analysis

4.1 FEM model

The experiment results showed that increasing of corner brace thickness could improve fatigue performance of roof weld, but stress variation of some certain points was unavailable in the lab. In this case, FEM models of steel bridge deck were established to analyse the local stress distribution and enhancement of fatigue performance due to the setting of corner braces. The stress distribution of corner braces was obtained and transfer of cracking position was verified by considering various structure parameters. Models of a steel deck with (CB) and without (NCB) were established (Nassiraei *et al.* 2016). The thickness of the roof was 16 mm and that of the pavement was 60 mm. Any slip between the deck and the pavement was ignored. The model considered seven *U*-ribs in the transverse direction and five cross-beams in the longitudinal direction, which had been proved to be accurate (Fu *et al.* 2016). As shown in Fig. 6, the corner braces were set at both sides of the *U*-ribs 4 in transverse direction and at the mid-span between the second and third diaphragms in longitudinal direction. Considering restraint conditions of the steel deck in the steel bridge as a whole, transitional DOF (degree of freedom) of roof and *U*-rib was restrained and both translational and rotational DOF of the diaphragm were restrained.

SHELL181 element were adopted for simulation of steel deck, *U*-rib, diaphragm and corner brace. SOLID185

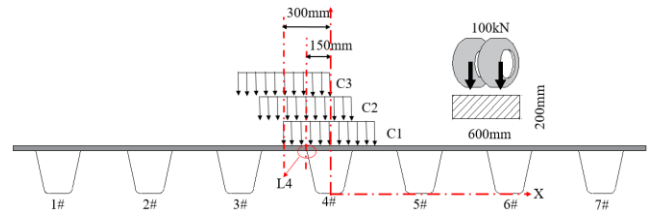
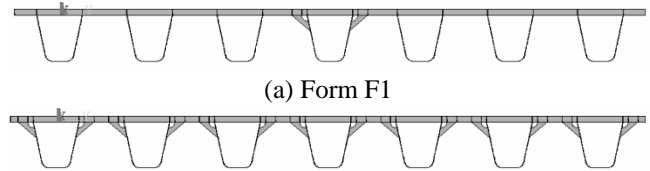


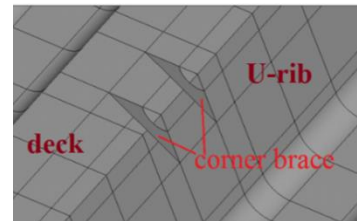
Fig. 7 Mesh grid of topographic model



(a) Form F1



(b) Form F2



(c) Form F3

Fig. 8 Arrangement forms of corner braces

element were adopted for pavement. The meshing was not carried out in thickness direction. Stress in CB section, i.e., section at the mid-span between the second and third cross-beams, was extracted, thus grids nearby were refined. 10 mm-size grids were adopted within 50 mm from CB section, 20 mm-size grids were adopted within 50 mm to 150 mm from CB section, 40 mm-size grids were adopted within 150 mm to 250 mm from CB section and 100mm-size grids were adopted beyond 250 mm from CB section. As the double wheel or the single wheel wouldn't influence the results in a qualitative manner, double-wheel loading to 100 kN was adopted. The loading area of wheels was simplified to a 600 mm length and 200 mm width rectangular area. The wheel load was applied to the section containing the corner braces. Three load positions in the transverse direction were considered (defined as C1 to C3, see Fig. 7). The *U*-ribs were numbered 1 to 7, from left to right, and load C1 was located on the centre of *U*-rib 7. Loads C2 and C3 had 150 mm and 300 mm eccentric offsets from load C1, respectively. In the figure, L4 indicated the left weld of *U*-rib 4 to the roof.

Three forms of arrangement, numbered F1 to F3, were considered as shown in Fig. 8. The thickness of the corner braces was 10 mm, the length was 100 mm, and the radius of the scallops was 35 mm. The corner braces were set at both sides of *U*-rib 4 in form F1 and at both sides of all *U*-ribs in form F2. In form F3, the two rows of corner braces, with a separation of 100 mm, were set at both sides of *U*-rib 4.

Three types of brace structural details, numbered CB1 to CB3, were considered as shown in Fig. 9. Detail CB1 had scallops on the braces with a 35 mm radius while detail 2 had no scallop. Detail CB3 had scallops on the low

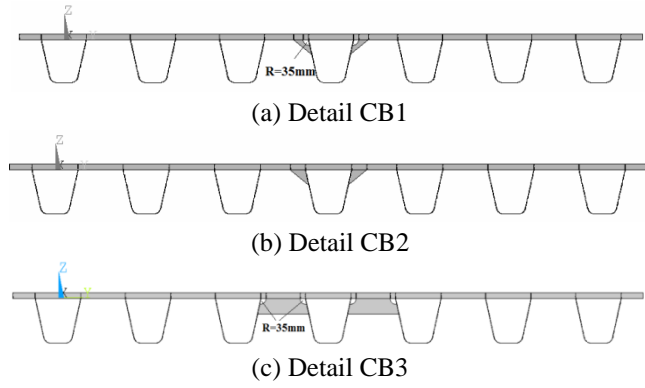


Fig. 9 Structural details: corner braces

transverse rib with a height of 100 mm between *U*-ribs.

4.2 Effects of the corner braces on stress distribution

Fig. 10 shows the transverse stress distributions on those steel decks with or without corner braces. Under load C1, the transverse stress distributions at the roof bottom were roughly similar no matter whether, or not, they included corner braces. The stresses near weld L4 were all about 56 MPa. Under load C2, the transverse stress distributions between *U*-ribs 4 and 5 were different. The maximum stress near weld L4 at the roof bottom, with corner braces, was -73 MPa and that without corner braces was -79 MPa. The corner braces caused a 7.6 % decrease in maximum stress near weld L4. Under load C3, the maximum stress near weld L4 decreased from -68 MPa to -58 MPa after setting corner braces. The transverse stress decreased by 14.7 %, which was greater than that under load C2. Therefore, corner braces decreased the maximum stress in the roof and *U*-rib weld under eccentric wheel loading applied in the transverse direction.

The stress distributions on left web of *U*-rib 4 with, and without, corner braces are shown in Fig. 11. The

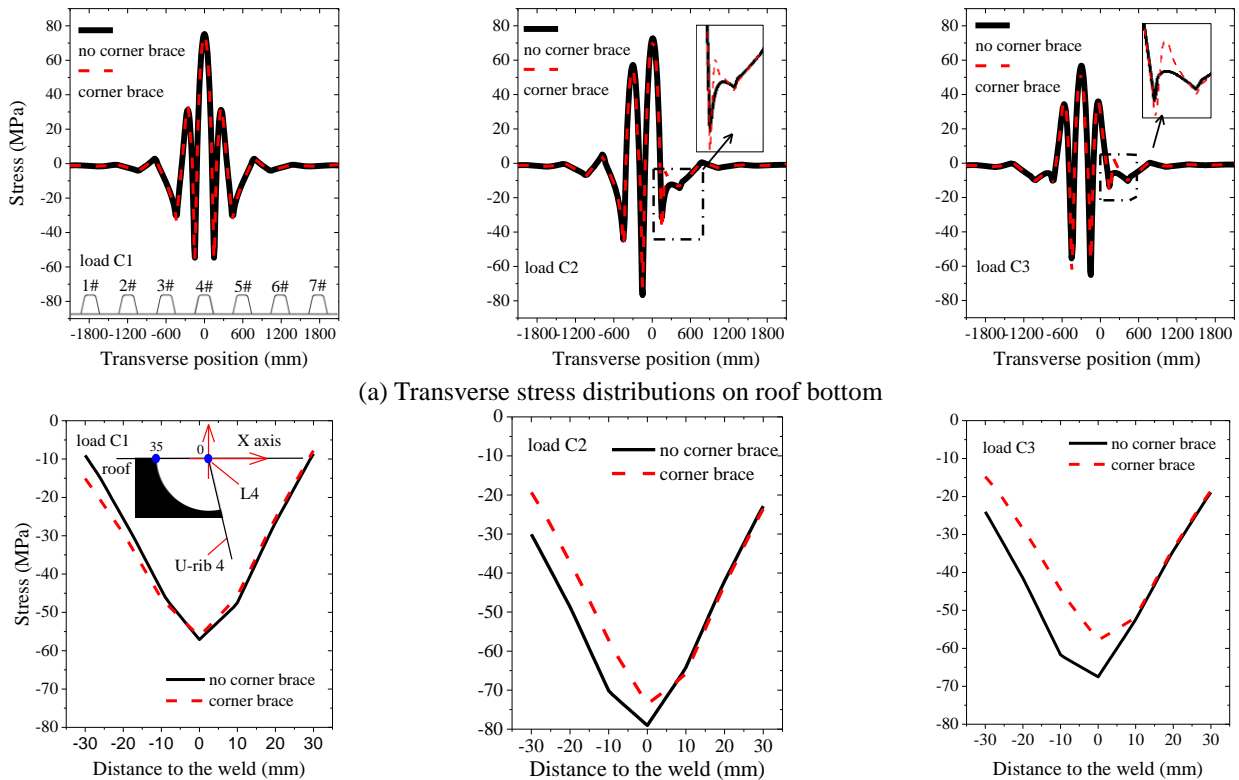


Fig. 10 Effects of the corner braces on the roof transverse stress

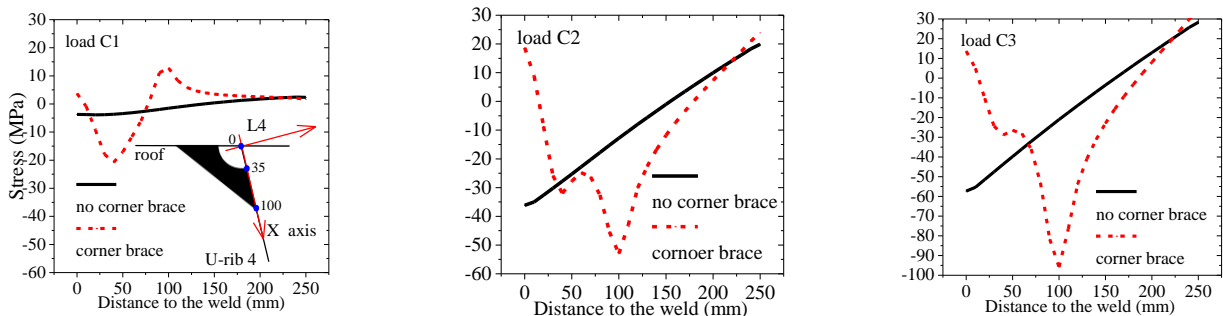


Fig. 11 Effects of corner braces on the stress in *U*-rib 4 (left web)

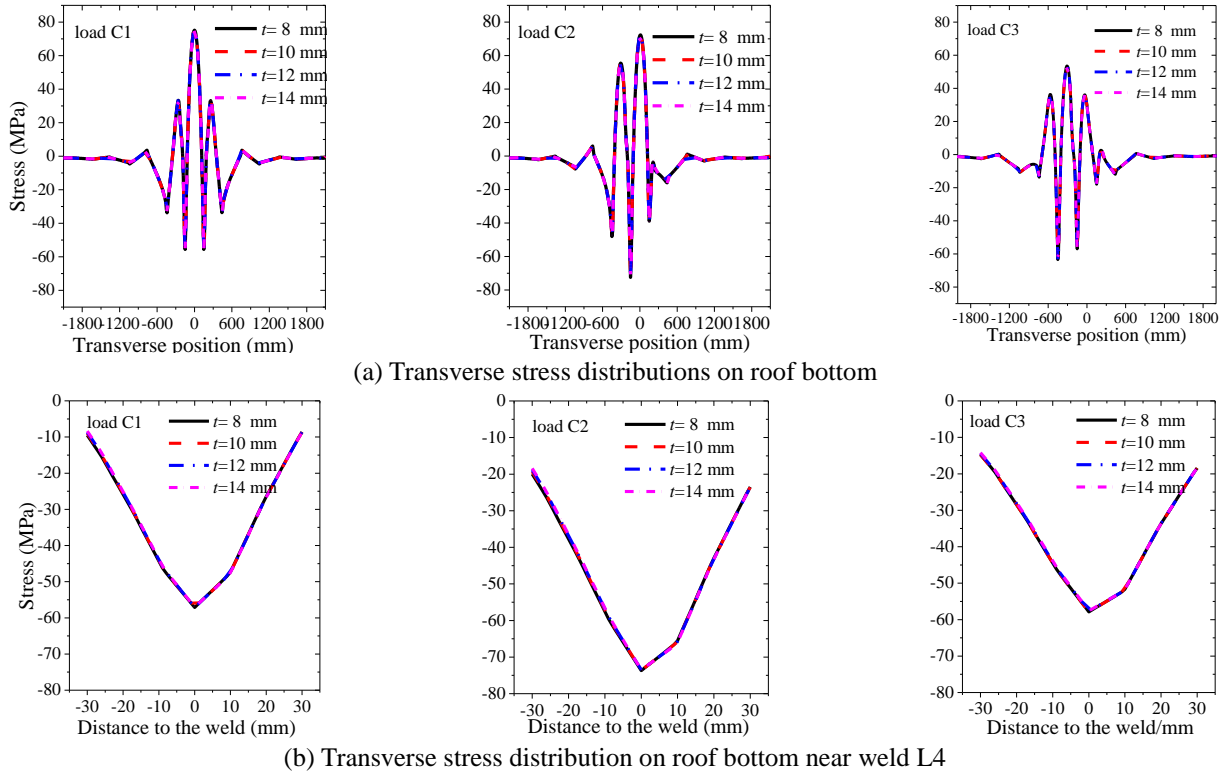


Fig. 12 Effects of the corner brace thickness on the roof transverse stress

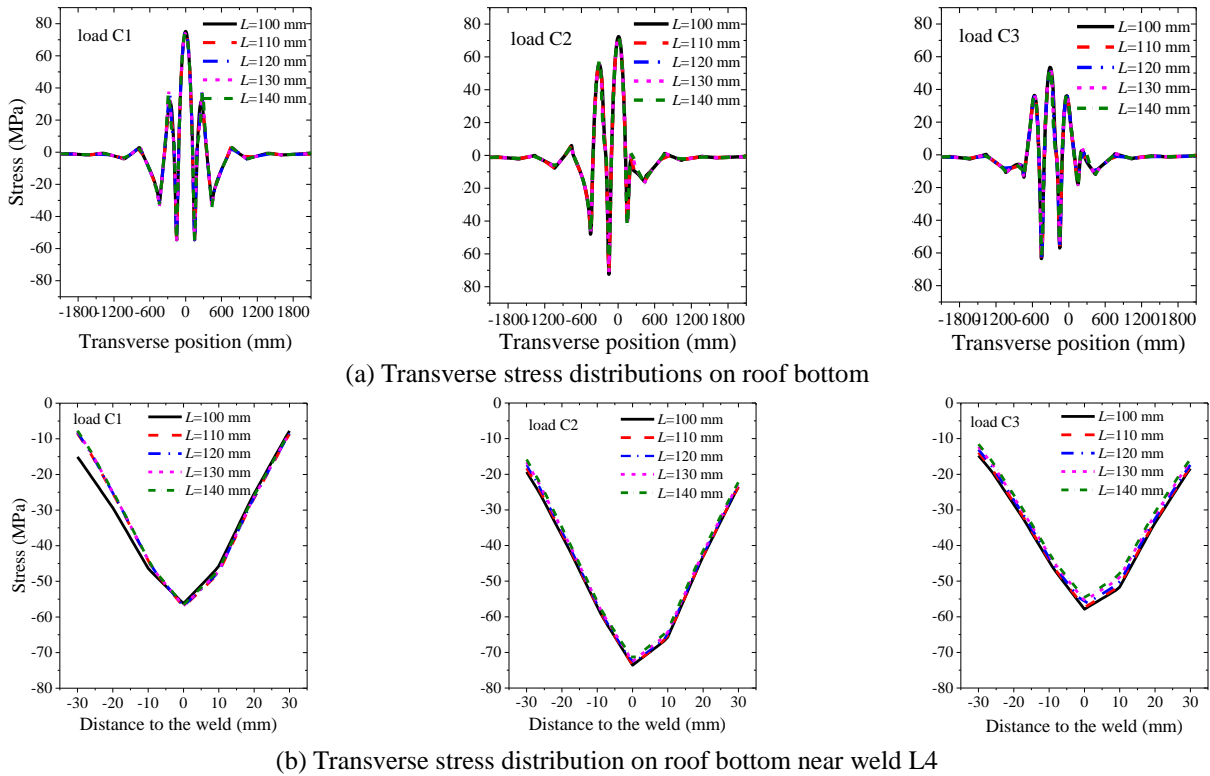


Fig. 13 Effects of the corner brace length on the roof transverse stress

stresses in the *U*-rib web were consistent with each other under different loading conditions and were distributed in an almost linear fashion when the deck had no added corner braces. The tops of the *U*-rib webs were subjected to compressive stress with maximum absolute values. The

compressive stress decreased and became tensile on a line from the web top to its bottom. The stress under load C3 was greater than that under other two loads. An eccentric load caused an increase in the web stress in the *U*-rib. For the deck with corner braces, the top of the *U*-rib web was

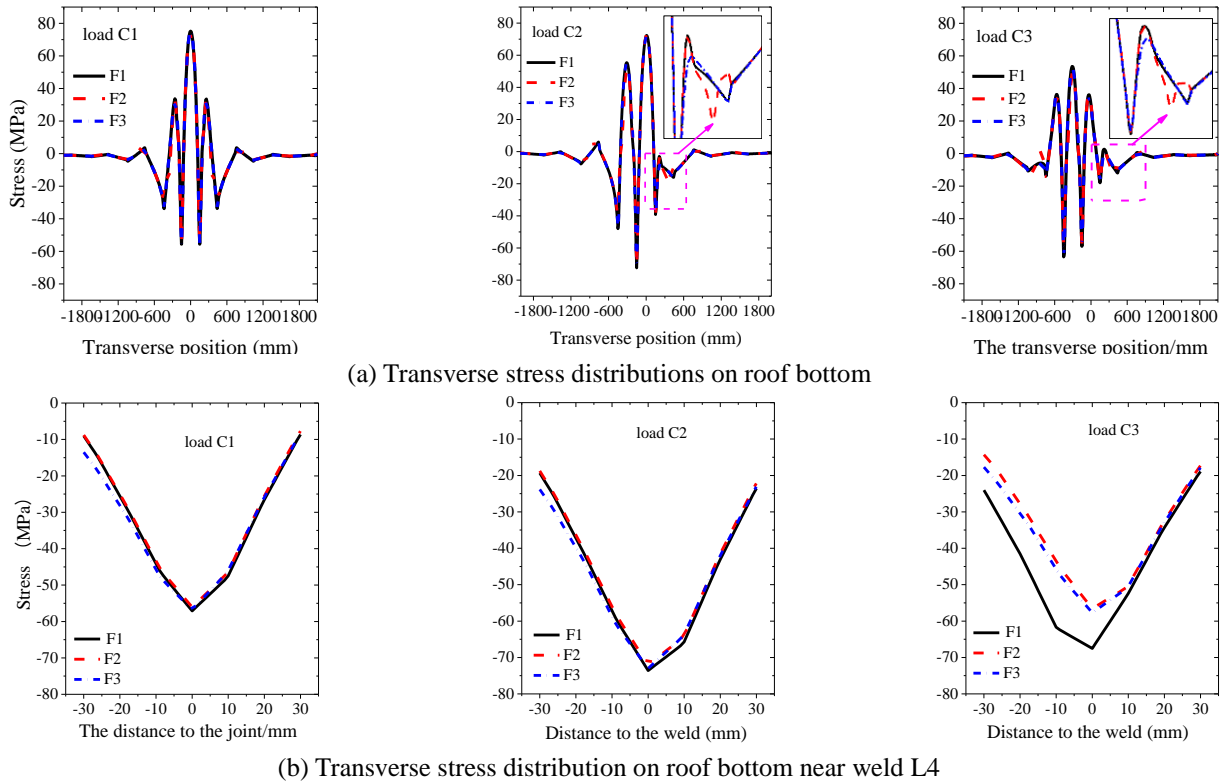


Fig. 14 Effects of the corner brace arrangement forms on the roof transverse stress

subjected to tensile stress. The stress decreased along the web from the top to its bottom, and changed from compressive to tensile at the bottom. Stress concentration occurred at the end of the corner braces. The corner braces turned the stress of the roof and *U*-rib weld toe on the *U*-rib web from compression to tension and caused this stress concentration. The stress on the roof was decreased while the stress on *U*-rib web increased; however, the decreased roof stress also decreased the probability of occurrence of a penetrating crack therein. The cracks on *U*-rib web were easier to detect and repair compared to a penetrating crack in the roof, therefore this was beneficial to bridge maintenance.

4.3 Effects of corner brace size

Fig. 12 shows the transverse stress distributions in steel decks with different corner brace thicknesses. The length of the braces was 100 mm and radius of the scallop was 35 mm. With increasing corner brace thickness, the transverse stress along the roof boom in a transverse direction, and in the *U*-rib web, remained unchanged which indicated that the corner brace thickness had no effect on the transverse stress distribution in the roof and *U*-rib weld. The effects of the corner braces were derived from, and related to, their vertical stiffness. Since the vertical stiffness was larger than that of the roof, the vertical stiffness change in the corner braces caused by an increase in their thickness had no effect on the stress distribution.

Fig. 13 shows the transverse stress distributions in a steel deck with corner braces of different lengths. The thickness of the braces was 10 mm and radius of the scallop

was 35 mm. The transverse stress distribution on the roof boom followed a similar trend. As shown in Fig. 13(b), the stress near weld L4 decreased slightly when the corner brace length increased. However, in general, the corner brace length had little effect on the transverse stress distribution in the roof and *U*-rib.

4.4 Effects of the corner brace arrangement

Fig. 14 shows the effects of different forms of corner brace arrangement. The corner braces sizes were 10 mm in thickness, 100 mm in length, and 35 mm in radius of the scallop. For arrangement forms F1 and F3, the transverse stress distribution curves on the roof bottom were almost the same, which meant that different numbers of corner braces along the weld had the same effect on the stress. However, the curves from analysis of arrangement form F2 were different from the other two between *U*-ribs 4 and 5 under an eccentric load. The tensile stress of F2 near the middle of *U*-ribs 4 and 5 decreased significantly compared to that of F1 and F3. The absence of corner braces on the right-hand side of *U*-rib 4 and left-hand side of *U*-rib 5 further enhanced the deck transverse stiffness at those positions. However, the stress from F2 on the roof bottom near *U*-rib 5 increased significantly due to the two weld ends which caused a more serious stress concentration than that of F1 and F3. The results indicated that setting corner braces on both sides of all *U*-ribs in the transverse direction increased the transverse stiffness, meanwhile, it also caused more serious stress concentration problems.

The load area centres of C1 and C2 were inside *U*-rib 4 and the stress distribution at the roof bottom near weld L4

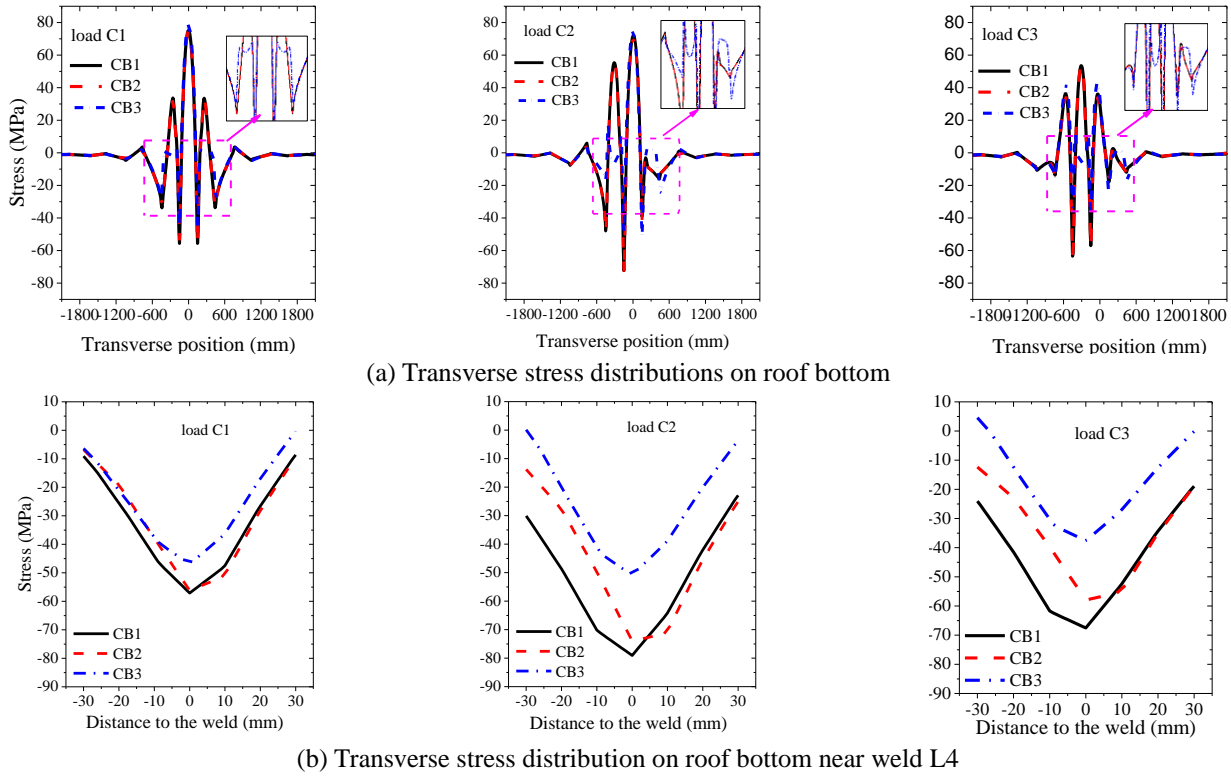


Fig. 15 Effects of the structural details on the roof transverse stress

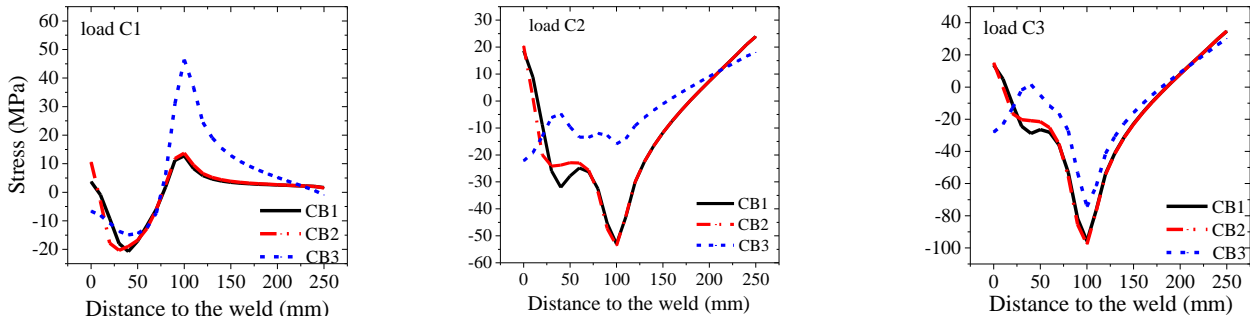


Fig. 16 Effects of structural details on the stress in *U*-rib 4 (left web)

were similar as shown in Fig. 14(b). The compressive stress varied linearly with slight differences between the three forms of arrangement and reached a maximum value at the toe of weld L4. The centre of load C3 was in the middle of *U*-ribs 3 and 4 and the trends in the transverse stress distributions for the three forms of arrangement were basically the same but with an obvious difference in the stress values. The transverse stresses at the roof bottom near weld L4 in forms F2 and F3 were lower by 18.9% and 15.3% (on average) than that in form F1. This indicated that the corner brace form of arrangement had no effects on the transverse stress on the roof bottom when the load centres were inside the *U*-rib. Otherwise, the transverse stress on the roof bottom decreased when the braces were set at more *U*-ribs as in form F2. The braces at other *U*-ribs nearby decreased the stress under an eccentric load.

4.5 Effects of the corner brace structural details

Fig. 15 shows the effects of different corner brace

structural details on the stresses. The sizes of corner braces and the low transverse rib were 10 mm in thickness, 100 mm in length, with a 35 mm scallop radius. The transverse stress distributions at the roof bottom for structural details CB1 and CB2 had the same trend, which reflected that scallops had no obvious effect on the transverse stiffness of the deck. Comparing the two other systems, the transverse stress at the roof bottom of structural detail CB3 decreased at both sides of *U*-rib 4 and the roof and *U*-rib welds. Therefore, low transverse ribs increased the transverse stiffness of the deck more than corner braces.

The transverse stress distributions on the roof bottom near weld L4 in Fig. 15(b) show that different details affected the stresses. The transverse stresses under load C1, when using details CB2 and CB3, were lower than when using CB1 by 5.6 % and 27.2 % on average. The decreases were 13.6 % and 52.6 % under load C2 and 18.5 % and 63.5 % under load C3. The comparison showed that scallops aggravated the local stress concentration. Therefore, scallops were not recommended when designing

corner braces of such decks, which matched the advice given for the design of cross-beams. The decreases in the transverse stresses near the weld by a low transverse rib were larger than that by corner braces, especially under eccentric load. Thus, a low transverse rib can be considered between the cross-beams to distribute the stiffness of the deck at some key positions, which can improve the local fatigue performance.

The effects of the corner brace structural details on the stress distribution at *U*-rib 4 (left web) are shown in Fig. 16. The curves for CB1 and CB2 almost coincided except within the 35 mm nearest the weld where there was a scallop in structural detail CB1. However, the stress in CB3 under load C1 increased at the underpart of the *U*-rib web. A maximum stress appeared on the curves at a position about 100 mm from the weld caused by the welded end of the corner brace. The value of the peak stress when using CB3 was about 50 MPa, while those with CB1 and CB2 were 15 MPa. Under loads C2 and C3, most of the left-hand *U*-rib web was subjected to a compressive stress. Between 35 mm and 100 mm from the weld, the compressive stress when using CB3, under loads C2 and C3, was lower than that found when using CB1 and CB2. Therefore, a low transverse rib had the beneficial effect of stress reduction in the *U*-rib web under eccentric load. While, the tensile stress under an axial load (load C1) at end of a brace increased when using CB3, which might have been a crack initiation position. However, the stresses at distances of less than 35 mm from the weld, when using CB3, were compressive and that found when using CB1 and CB2 were tensile, which was beneficial for the weld of roof and *U*-rib. It was worthwhile to change the crack's initial position from the roof weld to the *U*-rib web weld because of the difficulty inherent in any treatment of roof cracks.

5. Conclusions

Based on the study presented in this paper, the following conclusions are drawn:

- (1) Specimens with or without corner braces had similar crack contours. Local cracking caused stress redistribution but had no effect on the bearing capacity of the weld. The corner braces improved the stress distribution after cracking, which was beneficial in that it improved the fatigue performance.
- (2) The corner braces improved the transverse stress distribution in the roof while deteriorated that in the *U*-rib web. However, the decrease in roof stress reduced the probability of occurrence of a penetrating crack in roof. This was beneficial for bridge maintenance because of the difficulties inherent in the detection and repair of such cracks.
- (3) Because its vertical stiffness was large enough, the increase in corner brace sizes, and their number along the weld, had few effects on the stress distribution in the roof and *U*-rib weld. However, an increase in the number of corner braces along the transverse direction enhanced the overall stiffness of the deck, which was beneficial under an eccentric load and caused greater stress concentration.

- (4) Scallops were not recommended when designing corner braces of a deck according to the decrease of stress concentration when the braces without scallops were used. The decreases of stress near the weld near a low transverse rib were larger than those induced by corner braces, especially under eccentric load. Thus, a low transverse rib can be considered between the cross-beams to improve the local fatigue performance.

Acknowledgments

The research described in this paper was financially supported by the National Natural Science Fund of China (No.51678215, No.51678216) and the Fundamental Research Funds for the Central Universities (2015B17414).

References

- Aljabar, N.J., Zhao, X.L., Al-Mahaidi, R., Ghafoori, E., Motavalli, M. and Powers, N. (2016), "Effect of crack orientation on fatigue behavior of cfrp-strengthened steel plates", *Compos. Struct.*, **152**, 295-305.
- Colombi, P. and Fava, G. (2016), "Fatigue crack growth in steel beams strengthened by cfrp strips", *Theor. Appl. Fract. Mech.*, **85**, 173-182.
- De, F.B.P. and Kolstein, M.H. (2015), "Strengthening a bridge deck with high performance concrete", *Prog. Struct. Eng. Mater.*, **59**(4), 263-273.
- Fan, Y., Zhao, X. and Liu, Y. (2016), "Research on fatigue behavior of the flash welded joint enhanced by ultrasonic peening treatment", *Mater. Des.*, **94**, 515-522.
- Fu, Z.Q., Ji, B.H., Ye, Z. and Wang, Y.X. (2017a), "Fatigue evaluation of cable-stayed bridge steel deck based on predicted traffic flow growth", *KSCE J. Civil Eng.*, **21**(4), 1400-1409.
- Fu, Z.Q., Ji, B.H., Zhang, C.Y. and Li, D. (2017b), "Experimental study on the fatigue performance of roof and *u*-rib welds of orthotropic steel bridge decks", *KSCE J. Civil Eng.*, **22**(1), 270-278.
- Guo, T. and Chen, Y.W. (2013), "Fatigue reliability analysis of steel bridge details based on field-monitored data and linear elastic fracture mechanics", *Struct. Infrastr. Eng.*, **9**(5), 496-505.
- Ilman, M.N., Muslih, M.R., Subeki, N. and Wibowo, H. (2016), "Mitigating distortion and residual stress by static thermal tensioning to improve fatigue crack growth performance of mig aa5083 welds", *Mater. Des.*, **99**, 273-283.
- Japan Road Association (2002), *Guideline for Fatigue Design of Steel Highway Bridges*. (in Japanese)
- Ji, B.H., Liu, R., Chen, C., Maeno, H. and Chen, X.F. (2013), "Evaluation on root-deck fatigue of orthotropic steel bridge deck", *J. Constr. Steel Res.*, **90**(5), 174-183.
- Jua, X. and Tateishi, K. (2014), "Fatigue crack behavior at rib-to-deck weld bead in orthotropic steel deck", *Adv. Struct. Eng.*, **17**(10), 1459-1468.
- Kainuma, S., Yang, M., Jeong, Y.S., Inokuchi, S., Kawabata, A. and Uchida, D. (2016), "Experiment on fatigue behavior of rib-to-deck weld root in orthotropic steel decks", *J. Constr. Steel Res.*, **119**, 113-122.
- Kolase, P.K. and Desai, A.K. (2015), "Steel fiber reinforced concrete pavement: a review", *Int. J. Innov. Res. Sci. Technol.*, **1**(10), 274-276.
- Krejsa, M., Kala, Z. and Seitl, S. (2016), "Inspection based probabilistic modeling of fatigue crack progression", *Procedia*

- Eng.*, **142**, 145-152.
- Nassiraei, H., Lotfollahi-Yaghin, M.A. and Ahmadi, H. (2016), "Static strength of offshore tubular t/y-joints reinforced with collar plate subjected to tensile brace loading", *Thin Wall Struct.*, **103**, 141-156.
- Saberi, M.R., Rahai, A.R., Sanayei, M. and Vogel, R.M. (2016), "Bridge fatigue service-life estimation using operational strain measurements", *J. Bridge Eng.*, **21**(5), 04016005.
- Sakagami, T. (2015), "Remote nondestructive evaluation technique using infrared thermography for fatigue cracks in steel bridges", *Fatig. Fract. Eng. Mater. Struct.*, **38**(7), 755-779.
- Shao, X., Yi, D., Huang, Z., Zhao, H., Chen, B. and Liu, M. (2013), "Basic performance of the composite deck system composed of orthotropic steel deck and ultrathin rpc layer", *J. Bridge Eng.*, **18**(5), 417-428.
- Xie, F.X., Ji, B.H., Yuanzhou, Z.Y., Fu, Z.Q. and Ge, H.B. (2016), "Ultrasonic detecting method and repair technology based on fatigue crack features in steel box girder", *J. Perform. Constr. Facil.*, **30**(2), 04015006.
- Yang, M.Y., Ji, B.H., Yuanzhou, Z.Y. and Fu, Z.Q. (2016), "Fatigue behavior and strength evaluation of vertical stiffener welded joint in orthotropic steel decks", *Eng. Fail. Anal.*, **70**, 222-236.
- Zhang, S., Shao, X., Cao, J., Cui, J., Hu, J. and Deng, L. (2016), "Fatigue performance of a lightweight composite bridge deck with open ribs", *J. Bridge Eng.*, **21**(7), 04016039.